Meander Bend Evolution and Bank Erosion Modeling of a reach of Brahmaputra River, India using MIKE 21C Model

Kuldeep Pareta [1], Upasana Pareta [2]

1. DHI (India) Water & Environment Pvt. Ltd. Unit No. 339, Eighth Floor DLF Prime Tower. Okhla Phase-I, New Delhi - 110020. India.
2. Omaksh Consulting Pvt Ltd. D-632, 7th Avenue, Gaur City-1 Greater Noida, UP.

***Corresponding Author:**
Kuldeep Pareta

Email: kupa@dhigroup.com
Received: 2025.02.03
Accepted: 2025.05.25
J. Hydraul. Struct., 2026;12(4):14-41
DOI: 10.22055/jhs.2026.51623.1376

ABSTRACT

Riverbank erosion and rapid channel migration in large braided alluvial rivers such as the Brahmaputra pose substantial risks to infrastructure, settlements, and ecological systems. This study applies a high-resolution two-dimensional hydrodynamic and morphodynamic modeling framework to investigate meander bend evolution and bank erosion processes in an actively migrating reach near Palasbari, India. Simulations under bankfull and extreme flood conditions reveal pronounced hydraulic asymmetry within the bend, with peak velocities reaching 4.83 m s^{-1}, flow depths exceeding 65 m, and significant secondary circulation generating localized reverse flows greater than 3 m s^{-1}. These high-energy conditions produced deep local scour (>30 m) along the southern outer bank, confirming its high susceptibility to erosion during frequent and extreme flood events. Scenario-based intervention analysis demonstrates that sediment-guided realignment-through dredging of the mid-channel bar and strategic sediment placement along the outer bend-effectively reduces near-bank flow intensity and secondary currents, thereby lowering erosion potential. In contrast, structural flow deflectors intensified reverse flow zones and increased local instability, highlighting the risks associated with poorly evaluated engineering measures. The findings provide new process-based insights into meander morphodynamics under extreme hydraulic forcing and demonstrate the value of integrated hydrodynamic–morphodynamic modeling for evaluating erosion mitigation strategies. The study underscores the importance of adaptive, sediment-oriented river management approaches for sustaining morphological stability in highly dynamic alluvial systems such as the Brahmaputra River.

KEYWORDS

River morphology, erosion forecast, sediment transport, Brahmaputra River, MIKE 21C

1. Introduction

River morphodynamics refers to the interdisciplinary study of the physical processes that govern the evolution of river channels over time, driven by the complex interplay between water flow (hydrodynamics), sediment transport mechanisms, and channel bed and bank morphology [1, 2]. This field integrates principles of fluid mechanics, sedimentology, and geomorphology to understand how rivers respond to natural and anthropogenic forcings across varying spatial and temporal scales [3, 4]. Among river types, braided rivers exhibit the most dynamic morphodynamic behavior due to their network of multiple interlacing channels separated by transient mid-channel bars or islands [5, 6, 7].

These rivers are typically associated with high sediment supply, steep gradients, and variable discharge regimes, which together facilitate frequent channel avulsions, lateral migration, and bar formation or erosion [8, 9]. The inherent instability of braided systems makes them particularly sensitive to fluctuations in flow magnitude, sediment availability, and boundary conditions such as bank erodibility or vegetation cover [10, 11, 12]. Consequently, predicting morphological changes in these systems is a complex task with significant implications for river engineering, infrastructure resilience (e.g., bridge piers, embankments), flood risk management, and habitat conservation [13, 14, 15].

The Brahmaputra River exhibits highly dynamic hydro-sedimentary processes characterized by intense and recurrent channel migration, lateral bank erosion, and floodplain reconfiguration -phenomena that define its morphodynamic behavior [16, 17, 18]. The braided nature of the channel, with constantly shifting mid-channel bars and anastomosing threads, further compounds the river's unpredictability [19]. Satellite imagery observations and field surveys have reported riverbank erosion rates in the Brahmaputra River exceeding 72 m/year in certain reaches, causing significant land loss, population displacement, and damage to infrastructure [20, 21, 22]. Given the Brahmaputra's role in supporting densely populated floodplains, agrarian livelihoods, and key transport corridors, a robust understanding of its morphodynamics is imperative for sustainable river basin management [23, 24, 25, 26]

Historically, river morphodynamics were assessed using empirical techniques and 1D hydraulic models such as HEC-RAS or MIKE+, which, while foundational, are inherently limited in representing the spatial complexity and lateral variability of large braided rivers [11, 27, 28, 29, 30, 31, 32]. Empirical methods often rely on steady-state assumptions and uniform geometries that do not reflect the dynamic, non-linear nature of rivers like the Brahmaputra [33, 34].

Moreover, 1D models, which simulate flow along a longitudinal profile, fail to capture critical morphological processes such as bar formation, bifurcation, eddy formation, and localized bank erosion [10, 35, 36]. These limitations have led to the adoption of two-dimensional (2D) and three-dimensional (3D) models that provide spatially distributed and temporally responsive simulations of sediment dynamics, hydraulic flow, and morphological evolution [37, 38, 39, 40, 41, 42]. Among these, MIKE 21C - developed by DHI - has proven effective for braided and meandering rivers, offering advanced capabilities through its curvilinear orthogonal grid system, which conforms to natural river planforms and enhances model accuracy [43, 44, 45]. MIKE 21C integrates Saint-Venant equations with sediment continuity modules to simulate bed level changes, bar migration, lateral erosion, and sediment partitioning [46, 47, 48, 49, 50]. The model accounts for multiple sediment fractions and bank erosion processes driven by hydraulic shear and has been successfully applied in sediment-rich rivers such as the Brahmaputra, Ganges, and Mekong to support flood risk mitigation, river training design, and long-term morphological forecasting [32, 51, 52, 53].

Two-dimensional (2D) hydrodynamic and morphological modeling tools have proven highly effective for simulating sediment transport, erosion, and channel dynamics across varied riverine and coastal environments. Ramakrishnan [54] utilized the MIKE 21 Mud Transport model in the Gulf of Kachchh, leveraging Oceansat OCM-derived SSC to drive sediment simulations. The study emphasized the importance of tuning parameters such as settling velocity and critical shear stress based on sediment characteristics, revealing the spatial variability driven by tidal currents and seabed morphology. Morianou [43] applied MIKE 21C in the Koiliaris River and successfully reproduced water

levels and sediment transport using high-resolution DEMs and field data. Similarly, Dang [55] demonstrated the robustness of MIKE 21C in the lower Mekong River, capturing seasonal variations and sediment processes with strong calibration performance. In the Brahmaputra River, Karmaker [56] used a 2D model to simulate short-term morphological changes, validating thalweg shifts and evaluating groyne field effectiveness in braided systems. Morianou [57] extended these models to climate impact studies, highlighting that projected increases in rainfall could exacerbate bank erosion. Wang [58] modelled unsteady urban river flows using MIKE 21 FM, showing how cross-sectional irregularities affect hydraulic performance and flood risk. Pareta [59] applied MIKE 21C for predicting morphological evolution in the Brahmaputra, validating simulations with ADCP and flood-level data. These applications collectively highlight the reliability of 2D models in representing complex hydraulic and sediment transport processes for both natural and anthropogenic scenarios.

Recent studies have expanded the use of integrated 1D-2D modeling systems to improve sediment transport predictions and river management strategies. Pareta [32] developed a comprehensive framework combining MIKE Hydro River, MIKE 21 FM, and MIKE 21C to simulate hydrodynamic and sediment transport processes in the Banshadhara River. The model achieved high accuracy (98.3% for water levels, 86.7% for sediment transport), using the Wilcock & Crowe formula for gravel-bed conditions. The simulations revealed bend-induced erosion zones and spatially variable flow dynamics, supporting effective flood risk and channel migration assessments. In the sediment-laden Brahmaputra River, Pareta [53] further employed MIKE 21C to forecast morphological evolution. Validation with ADCP observations confirmed the model's reliability in scenario-based erosion prediction and design of training works. Le [60] assessed coastal morphological responses to breakwaters in the Mekong Delta using MIKE 21 FM, illustrating how optimized breakwater configurations enhance sediment deposition and shoreline stabilization. Sarker [61] combined 1D and 2D techniques to distinguish floodplain from channel flows, improving risk analysis in low-gradient terrains. Samir [62] modelled flow disruptions during bridge rehabilitation on the Nile, showing that reduced cross-sectional areas can alter hydrodynamics, advocating for low-flow period interventions. Jiang [63] introduced the AHMS-SED model in the Yellow River Basin to couple hydrology with sediment transport, successfully reproducing gully erosion trends under climatic and human-induced changes. These efforts underscore the growing sophistication of modeling frameworks in supporting sediment management, infrastructure design, and adaptive river basin planning.

This study aims to employ the MIKE 21C modeling framework to simulate and morphological forecast and bank erosion in a selected reach of the Brahmaputra River. The specific objectives include: (i) development and calibration of a 2D morphological model for the target reach; (ii) analysis of hydraulic behavior and morphological dynamics at the south bank hill bend; (iii) simulation of sediment transport and channel evolution under varying hydrological conditions; (iv) projection of future morphological changes, including general and bend scour development; and (v) identification of erosion-prone zones to inform riverbank protection and management strategies.

2. About the study area

Figure 1 depicts the location of the study reach and highlights the key surrounding locations within the study area.

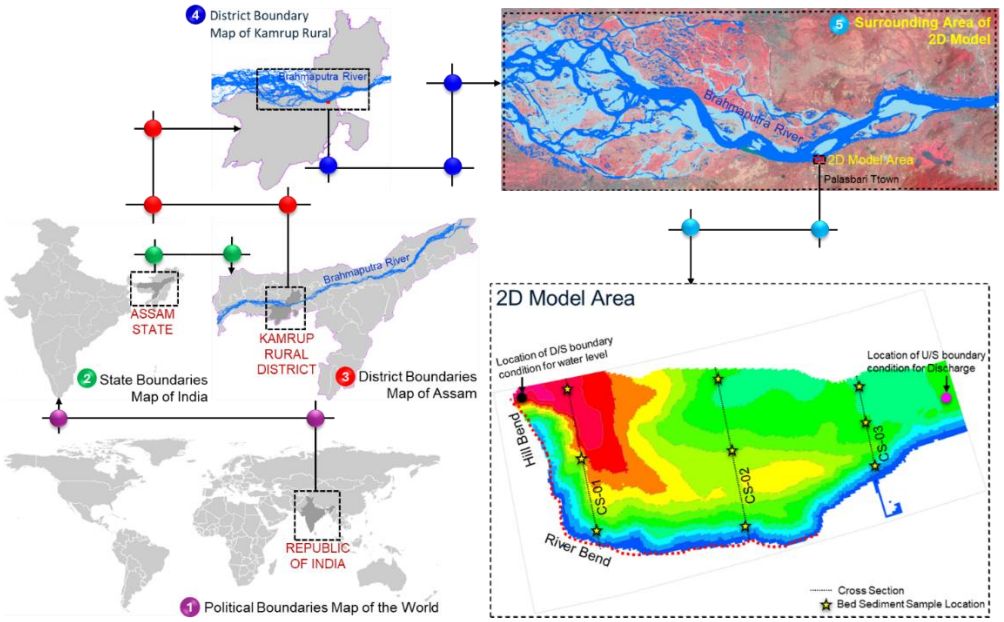
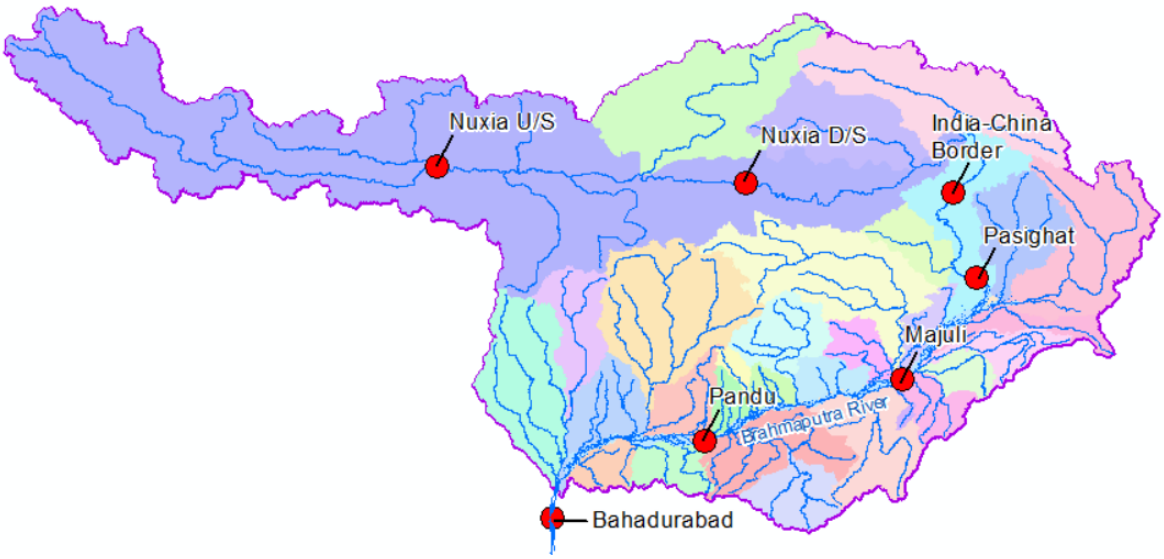


Figure 1. Location map of study area showing hill bend near Palasbari town of Assam state, India

The Brahmaputra River, one of the largest and most sediment-laden rivers in the world, presents a quintessential example of the complexities associated with morphodynamic processes in braided river systems [23, 64, 65]. Originating from the Manasarovar Lake region, near Mount Kailash in the Tibetan Himalayas, the river traverses a highly varied topography and climatic regime as it flows through China (as Yarlung Tsangpo), enters India through Arunachal Pradesh, and meanders through the alluvial plains of Assam before entering Bangladesh [66, 67]. Throughout its course, particularly in the middle reaches across northeastern India, the river is subject to extreme seasonal hydrological variability [68, 69, 70]. This is largely driven by the South Asian monsoon, during which the Brahmaputra experiences substantial increases in discharge, often exceeding 22,000 m^3/s, accompanied by an enormous sediment influx derived from steep, erosion-prone Himalayan catchments [71, 72, 73]. The mean annual flow of the Brahmaputra River system exhibits significant spatial variability across different gauging stations, ranging from approximately 31,200 million cubic meters per year (MCM/yr) to 605,490 (MCM/yr) (Table 1). The annual sediment load of Brahmaputra River has been estimated at over 400 million tonnes / year, placing the river among the highest sediment-yielding systems globally [65, 74, 75].

Table 1. Mean annual flows at key locations along the Yarlung Tsangpo–Brahmaputra–Jamuna River System

S. No.	River reach	Observation site	Mean flow (MCM/yr)	References
1	Yarlung Tsangpo	Nuxia U/S	31,200	[76]
2	Yarlung Tsangpo	Nuxia D/S	60,570	[77]
3	Yarlung Tsangpo	India-China Border	135,900	[77]
4	Siang	Pasighat	185,100	[78]
5	Brahmaputra	Majuli	278,447	[79]
6	Brahmaputra	Pandu	526,100	[80]
7	Jamuna	Bahadurabad	605,490	[76]



Mean annual flow observation sites along the Yarlung Tsangpo–Brahmaputra–Jamuna River System

The hill bend at the study reach is a prominent geomorphological feature along the southern bank of the Brahmaputra River, located in the Kamrup Rural district of Assam, India, near the town of Palasbari. Geographically, the reach spans between 26°07'02.302"N to 26°07'13.661"N latitude and 91°31'06.476"E to 91°31'39.092"E longitude (Figure 1), approximately 20 km southwest of Guwahati. This bend is distinguished by a pronounced curvature adjacent to a stable hill slope, which exerts a substantial influence on the river's hydrodynamic and morphodynamic behavior. The proximity of elevated terrain along the concave (outer) bank confines the channel laterally, enhancing flow acceleration and concentrating shear stress during high discharge events. Consequently, the bend experiences intensified bank erosion and scour development along its outer margin. The restricted lateral mobility due to the hill's presence makes this reach especially vulnerable to hydraulic forces, thereby classifying it as a high-priority zone for riverbank protection and river training interventions. The strategic significance of this bend is further amplified by its proximity to densely populated areas and critical infrastructure, necessitating informed and sustainable morphological management.

The study reach is characterized by a humid subtropical climate, with an average annual rainfall of approximately 2,300 mm (Shing et al., 2004). The mean annual temperature is around 24°C, with minimum temperatures reaching 17°C during the winter months (December to February) and maximum temperatures rising to 39°C in the summer (June to August).

3. Data used

3.1. Digital elevation model and bathymetric data

Copernicus digital elevation model (DEM) a 30 m resolution Digital Surface Model derived from the WorldDEM dataset via the TanDEM-X mission (DLR and Airbus), represents surface features including vegetation, infrastructure, and built-up areas. In this study, Copernicus DEM (2015), sourced from the Copernicus Data Space, was utilized to validate cross-sectional elevation profiles and support detailed topographic analysis of the study area.

Cross-sectional data utilized in this study were obtained from the Water Resources Department, Assam. These datasets were further refined and enhanced through the integration of available bathymetric

measurements to improve the representation of channel geometry and subaqueous features.

Gridded bathymetric data employed in this study were sourced from the General Bathymetric Chart of the Oceans (GEBCO), specifically the GEBCO_2024 Grid-a global terrain model that provides elevation information for both terrestrial and oceanic surfaces. This dataset, available at 15 arc-second (~400 m) spatial resolution, is accompanied by a Type Identifier (TID) Grid, which classifies the underlying sources used in the generation of elevation values. Bathymetric data spanning the period from 2019 to 2024 were downloaded from the GEBCO repositoryto support topographic and morphological analyses within the study area.

3.2. Hydrological and meteorological data

Gridded river discharge data utilized in this study were sourced from the Copernicus Emergency Management Service (CEMS) Early Warning Data Store, specifically from the Global Flood Awareness System (GloFAS). These data are generated using the LISFLOOD hydrological model, which is forced with ERA5 meteorological reanalysis inputs interpolated to a spatial resolution of 0.05° (approximately 5 km) and produced at a 24-hour temporal resolution. GloFAS provides two types of hydrological outputs: intermediate data, derived from the near real-time ERA5T inputs and updated daily, and consolidated data, based on the finalized ERA5 reanalysis and updated monthly. For the present study, daily river discharge data spanning the period 2015 to 2024 were acquired and used to analyze hydrological dynamics within the study reach. The dataset was used for both simulations. The 2-year and 100-year return period floods were computed using statistical frequency analysis of the observed flow data, applying the standard hydrological methods (e.g., Gumbel's extreme value distribution).

Water level observations for the period 2015-2024 were obtained from the Central Water Commission (CWC). These data provide critical insights into the temporal fluctuations of water levels in the study area and were utilized to support hydrodynamic modeling and river behavior analysis.

3.3. Bed sediment sample

In December 2024, a total of nine bed sediment samples were collected using a Van Veen Grab sampler from three cross-sections within the 2D model domain to analyze grain size distribution, gradation, and sorting (Figure 1). The samples were specifically collected to assess hydraulic roughness and sediment transport characteristics. At each cross-section, one sample was taken from the mid-channel, and two samples were collected from the bank-adjacent areas. These data are essential for understanding the sediment dynamics and refining the model's sediment transport predictions.

3.4. Satellite and ancillary data

Satellite imagery from Landsat-5 TM, Landsat-7 ETM+, Landsat-8 OLI, and Landsat-9 OLI-2, each with a spatial resolution of 30 meters, covering the period from 2013 to 2024, were obtained from Earth Explorer. These images were employed for the analysis of river planform, riverbank erosion, and delineation of banklines, providing critical data for understanding morphological changes in the study area.

3.5. Data limitations

Despite the use of reliable and widely accepted datasets, certain limitations were inherent in the input data utilized for this study. The Copernicus DEM, with a spatial resolution of 30 m, may include surface features such as vegetation and built-up infrastructure, potentially leading to overestimated elevations in densely vegetated or urbanized areas. To mitigate this, cross-sectional elevation data from the Water Resources Department, Assam, were

used to validate and refine terrain representation. Similarly, GEBCO bathymetric data, available at ~400 m resolution, lack the spatial detail necessary for fine-scale channel morphology representation and were therefore enhanced using in-situ bathymetric and cross-sectional measurements where available. The GloFAS discharge dataset, while offering consistent and long-term gridded hydrological data, represents modelled outputs and may not fully capture localized flow variability, particularly in complex alluvial systems like the Brahmaputra. To address this, observed water level data from the Central Water Commission (CWC) were used for calibration and validation of hydrodynamic simulations. Furthermore, satellite imagery analysis using multi-temporal Landsat data (2013-2024), with a spatial resolution of 30 m, is affected by seasonal cloud cover and varying river stages, which may obscure banklines and charland features. These limitations were addressed through careful image selection and cross-verification using ancillary datasets. While these measures enhance data reliability, the inherent limitations may still introduce uncertainties in model outputs, particularly in regions with sparse observations or highly dynamic morphological features.

4. Methodology

4.1. Overview of numerical modelling tools

Two-dimensional numerical models are effective tools for simulating long-term river morphology and assessing the influence of river engineering structures. A benchmarking study conducted by the National Sedimentation Laboratory (ARS-USDA) for the U.S. Army Corps of Engineers [81] evaluated the capabilities of such models. Among several candidates, only five met the established criteria: MIKE 21C (DHI, Denmark), Delft2D-Rivers (Deltares, Netherlands), CCHE2D (NCCHE, University of Mississippi, USA), TABS-MD (US Army Corps of Engineers, USA), and TELEMAC (EDF, France). Of these, MIKE 21C and Delft2D demonstrated the most comprehensive theoretical frameworks for modeling sediment transport, bank erosion, and morphological evolution in curved river channels. A comparison of their key features is summarized in Table 2.

Table 2. Salient features of MIKE 21C and Delft2D for two-dimensional hydrodynamic and sediment transport simulations

S. No.	Key features	MIKE 21C	Delft2D
1	Governing equations solved in curvilinear finite difference gird	✓	✓
2	Time integration method is second order, thus accurate and allows larger time step, computation is efficient	✓	✓
3	Capable of wetting and drying, very important in braided rivers	✓	✓
4	Temporal and spatial variation in use of flow roughness, very important in braided rivers	✓	x
5	Simulate non-cohesive bed material separately for bed and suspended load by different size class, and erosion/deposition of riverbed	✓	✓
6	Simulating transport, erosion, deposition and consolidation of cohesive materials	✓	✓
7	Simulate transport of sand and mud mixtures	✓	x
8	Include effects of helical flow in river bends on momentum and sediment load	✓	✓
9	Bank erosion in fixed and in moveable grid	✓	x

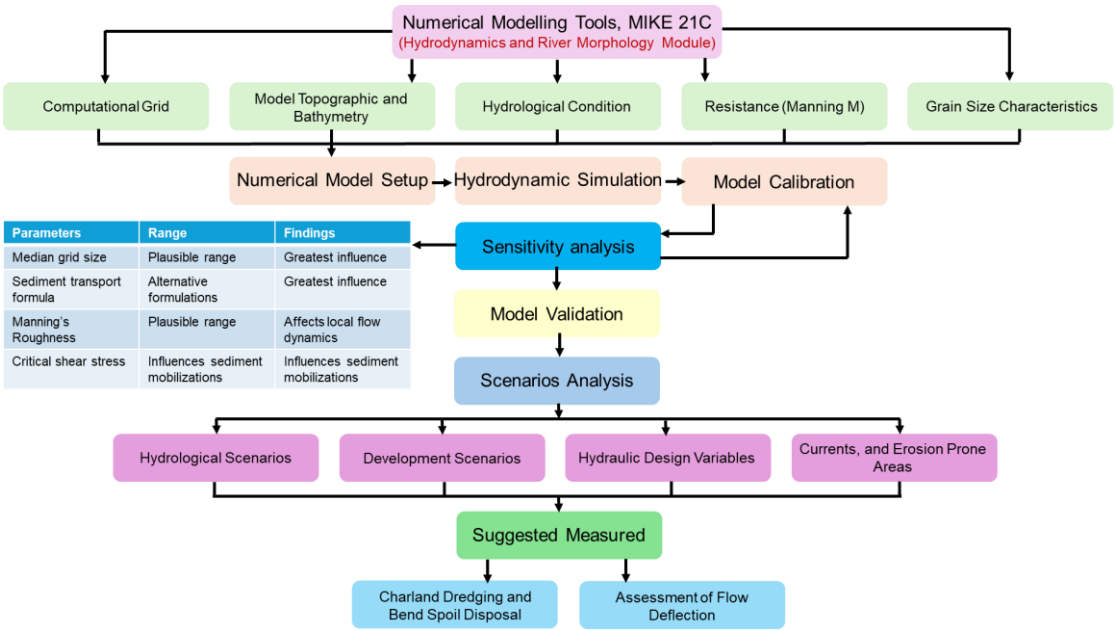


Figure 2. Schematic workflow of the methodology for 2D hydrodynamic and morphodynamic modeling.

MIKE 21C was selected for its advanced capabilities in simulating complex fluvial systems, particularly braided river reaches. Its use of a flexible curvilinear grid allows for precise representation of natural channel geometry with minimal grid distortion. In contrast to Delft2D, which employs structured or unstructured grids, MIKE 21C offers enhanced efficiency in modeling sediment transport dynamics, bank erosion processes, and long-term morphological evolution. This makes it particularly suitable for detailed, process-based analyses required in river engineering and sediment management applications. A schematic workflow of the methodology and modeling framework is shown in **Error! Reference s ource not found.**.

4.2. Model setup and input data

4.2.1. Computational grid

A two-dimensional hydrodynamic model of the study reach near the hill bend was developed using 7,860 computational cells within a curvilinear orthogonal grid framework in the MIKE 21C modeling system. The domain spans approximately 1 km in length and 0.5 km in width, comprising 120 cells along the flow direction and 65.5 cells across the channel. The curvilinear grid enables variable cell dimensions, with an average longitudinal cell size of about 7.5 meters, allowing efficient representation of complex channel geometry (Figure 3). A detailed mesh convergence test was conducted to ensure numerical accuracy and solution stability. Multiple grid resolutions were evaluated, and key hydraulic and morphological outputs-such as velocity distributions, bed level changes, and water surface profiles-were compared. Convergence was confirmed when changes in results between successive mesh refinements became negligible (within 5%). This high-resolution configuration was found to be optimal capturing localized morphological dynamics such as bend scour, obstruction-induced scour, and bank erosion with sufficient precisions. The model's capability was validated through bathymetric outputs, which successfully depict the observed scour zones near the hill toe with well-defined depth contours.

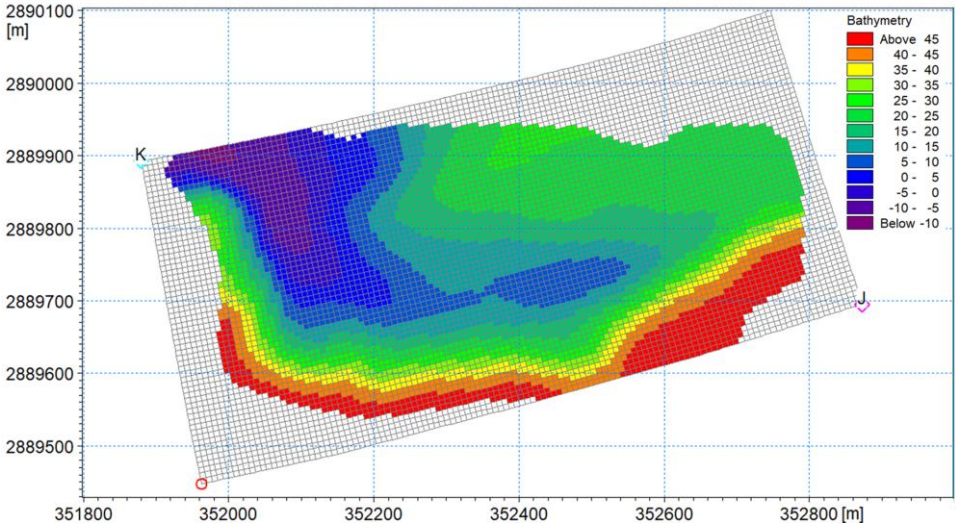


Figure 3. Curvilinear grid configuration and bathymetric profile of the hill bend study reach near Palasbari town.

4.2.2. Model topography and bathymetry

The bathymetry for the two-dimensional model was developed using a combination of gridded bathymetric datasets (2019-2024) and high-resolution cross-sectional data. Approximately 40 cross-sections were collected over a 1 km stretch along the thalweg, capturing the channel's deepest zones. The integrated dataset enabled the construction of a detailed bathymetric surface within the model domain, as illustrated in Figure 3. The resulting bathymetry effectively resolves morphological features such as scour zones, particularly in the vicinity of the hill bend, owing to the fine spatial resolution of the computational grid and the high accuracy of the survey inputs.

4.2.2. Hydrological condition

The boundary conditions for the present localized hydrodynamic model were derived from a large-scale model framework [82]. The upstream inflow boundary was specified using discharge data from the Pandu gauging station, while the downstream boundary was defined by applying observed water level data. Model calibration was performed using data from the 2023 hydrological year (Figure 4), and subsequent validation was carried out in June 2024. Discharge at the Pandu station for the calibration period was estimated through a stage–discharge relationship established via a rating curve based on observed water level measurements.

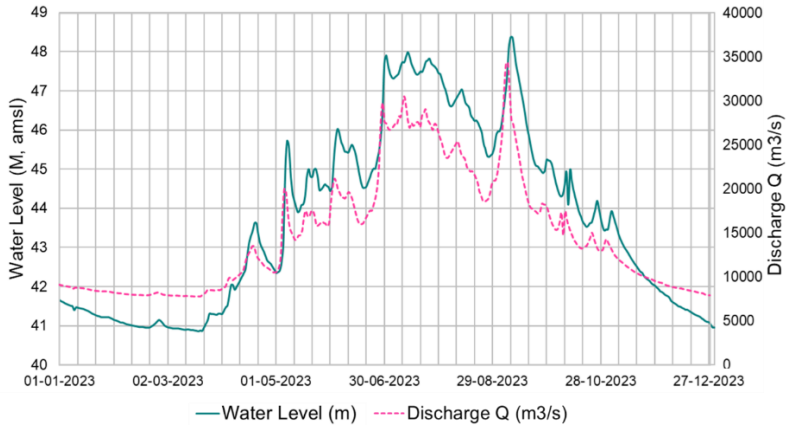


Figure 4. Two-dimensional model boundary conditions, inflow discharge and downstream water

level at Pandu gauging station.

At the Pandu gauging station, the bankfull discharge is approximately 42,500 m³/s, while the corresponding bankfull discharge incorporated from the large-scale model into the local model domain is about 10,073 m³/s. The 100-year flood discharge at Pandu is estimated at 66,000 m³/s, whereas the large-scale model provides a value of approximately 16,943 m³/s for the local reach. A continuous time series of discharge at Pandu was reconstructed from daily water level records using empirically derived stage–discharge rating relationships (Eq.1 and Eq.2). These relationships were developed based on observed water levels and corresponding discharge measurements from the 2014 hydrological year, which captured a comprehensive range of flow conditions, including near-bankfull stages. The Pandu gauging site is located within a geomorphologically stable reach of the Brahmaputra River, rendering the rating curves robust and valid across the recent decade (2015-2024). The established rating curves have also demonstrated reliable predictive capability for extreme hydrological events, including the 2-year (bankfull), 50-year, and 100-year return period discharges [53, 83, 84]. The 2-year (bankfull), 50-year, and 100-year return period discharges were estimated using established rating curves, developed from observed stage-discharge data at the Pandu gauging station for the period 2000-2023. Frequency analysis using the Gumbel distribution was then applied to the rating curve-derived discharge values to estimate the return period floods. These rating curves have demonstrated reliable extrapolation capability for extreme events.

Two rating curve equations were employed to estimate discharge at the Pandu gauging station, segmented by stage height.

Stage-I rating curve, valid for water levels up to 47.13 m amsl, is expressed as:

$$h = 14.163 \times Q^{0.1182} \quad (1)$$

Stage-II, applicable for water levels exceeding 47.13 m amsl, is defined as:

$$h = 23.923 \times Q^{0.0673} \quad (2)$$

Where h is the water level (m amsl) and Q is the discharge (m³/s).

Although refinement of the rating relationship for low-flow conditions (Q < 10,000 m³/s) during the dry season was feasible, such enhancements were deemed less critical given the focus on simulating flood-induced morphological changes. Nevertheless, the rating curve was optimized as part of the model calibration process. Ideally, the downstream boundary conditions of the 2D model would rely on observed stage data. However, in the absence of a gauging station in proximity to the downstream boundary-aside from the Pandu station-water level inputs were extrapolated to this location. This introduces a degree of uncertainty in the model outputs. To address this, a boundary sensitivity analysis was performed to evaluate the influence of downstream conditions on model performance and improve reliability.

4.2.4. Grain size characteristics

The collected samples were conducted using a Van Veen grab sampler, adhering to established procedures [85, 86]. Sieve analysis [87] was employed to quantify the sediment size classes, including the median grain diameter (D_{50}), which are presented in Table 3. The observed grain size data align well with published values for the Brahmaputra River, further validating the field measurements.

Grain sorting, evaluated through the sorting coefficient (σ), revealed well-sorted sediment across the sampled reach. Values of σ were consistently below 1.6, indicating a uniform sediment distribution as defined by established thresholds [46, 88]. Such uniformity justifies the use of sediment transport equations that assume a single representative grain size (D_{50}), thus improving the reliability of sediment transport and morphological modeling in the 2D simulation framework (Table 3).

Table 3. Grain size characteristics of bed material in the study reach (field data) and the Brahmaputra River (from literature).

S. No.	Grain class	Study reach*	Brahmaputra in Assam**	Brahmaputra in Jamuguri***
1	D_{16} (mm)	0.15		
2	D_{50} (mm) #	0.24	0.25 to 0.16	0.16
3	D_{65} (mm)	0.29		
4	D_{84} (mm)	0.44		
5	σ (grain sorting parameter, $(D_{84}/D_{50})^{0.5}$	1.65		

* Grain size distribution (median size class, see note below) of the sediment samples collected by Author.
* All the grain size distribution (GSD) values are averaged across the three cross-sections.
** Grain size range [89].
*** Grain size at Jamuguri [90].
# The D_{50} values in the table are arithmetic means of D_{50} values of all samples from respective river reach.

4.3. Sensitivity analysis

A sensitivity analysis was performed to assess the impact of key input parameters on sediment transport and morphological evolution in the MIKE 21C model. Parameters tested included median grain size (D_{50}), sediment transport formula, Manning's roughness coefficient, and critical shear stress for erosion and deposition. Each was varied within plausible limits derived from field data and literature, while keeping others constant [91, 92]. Model responses were evaluated in terms of changes in bed elevation, sediment flux, and scour depth.

The analysis revealed that sediment transport formula selection and D_{50} exert the greatest influence on predicted erosion and deposition patterns [30]. Manning's roughness primarily affected local flow dynamics, while critical shear stress influenced sediment mobilization thresholds under moderate flows [93]. These findings highlight the necessity of accurate field calibration to ensure reliable morphological forecasting in braided and dynamic riverine systems.

4.4. Scenarios and calibration

4.4.1. Hydrodynamic and erosion prediction

Hydrodynamic and erosion prediction involves simulating flow dynamics and sediment transport to identify erosion-prone zones and assess morphological changes. This helps evaluate the impact of hydraulic structures and flow variations on channel stability.

Hydrological scenarios: Hydrodynamic simulations were conducted under varying hydrological conditions to predict key design parameters along the study reach. The modeling focused on the monsoon season, characterized by heightened morphological activity. Two primary flood scenarios were evaluated: (i) the bankfull discharge condition, representing an event with an approximate 2-year return period, and (ii) the extreme 1 in 100-year flood condition. Discharge and water level hydrographs from the 2023 monsoon season (Figure 4) were used as a baseline and subsequently scaled to reflect the peak magnitudes associated with these design flood scenarios.

Development scenarios: For morphological forecasting, the above hydrological condition has been used, the condition / scenario for morphological prediction was as follows: (i) full length of the south bank of study reach was considered non-erodible, similar to assumption the banks are trained/fixed; aim is to assess scour development in the river, and will allow to

see extreme development useful for assessing dimension of protection work into the river, and volume of protection material; model will assess the magnitude of scour. However, the calculation of the volume of protection material or size of material / rock / boulder is intended to be calculated after adding local scour depth to the scour predicted by the 2D model; (ii) the river training work at upstream of study reach was set-up in the model, i.e., existing protection work immediate upstream of damaged study reach is considered as fixed, i.e., non-erodible bank, and thus, impact on bank erosion of the damaged bend reach on south bank has been assessed.

Hydraulic design variables: The hydraulic simulations for design variable estimation were conducted under fixed-bed conditions, based on the most recent riverbed topography of 2024. Two hydrological scenarios were considered: (i) bankfull discharge corresponding to a 1-in-2-year return period, and (ii) an extreme flood event with a 1-in-100-year return period. Depth, velocity, and water level distributions around the damaged study reach were computed relative to the 2024 bathymetry. While flow depth is sensitive to temporal variations in riverbed morphology, water levels remain relatively stable under consistent hydrologic inputs. Therefore, the water levels reported in Table 4 can be applied to estimate depth for other recent topographic conditions. The depth-averaged velocities values, as presented, exhibit minimal sensitivity to minor bed level changes. A comprehensive summary of the computed hydraulic variables is provided in Table 4. It is important to emphasize that the total design scour depth must include both general and local scour components. The current 2D MIKE 21C model framework is also recommended for evaluating the hydraulic performance of proposed riverbank protection measures such as revetments, geo-bags, or spurs.

Currents, and erosion prone areas: The study reach, characterized by an active meander bend, exhibits significant morphological dynamics, with both primary and secondary flow components playing critical roles in driving erosion processes. Under bankfull discharge conditions - which occur with relatively high frequency - the model predicts primary flow velocities exceeding 2 m/s, with peak velocities reaching approximately 3 m/s. This generates strong flow circulation and reverse flows in the downstream portion of the bend, with reverse velocities also exceeding 2 m/s (Figure 5 A). Given that the critical threshold for initiating sediment motion for 0.24 mm sand is approximately 0.1 m/s, such frequent high-flow conditions are sufficient to induce substantial bed scour and bank erosion. The presence of strong secondary currents further exacerbates these processes; the prevailing secondary flows are directed away from the bank (i.e., in the positive direction), which intensifies lateral sediment transport and enhances scouring along the outer bank (Figure 5 B). The current speed (Figure 5 C), and bed level map (Figure 5 D) confirms the persistence of a pronounced scour hole (bed elevation below -5 m) near the toe and head of the hill at the study reach. There is no indication of sediment deposition or natural infilling in this zone, suggesting that erosional processes will continue to dominate the morphological evolution of this bend.

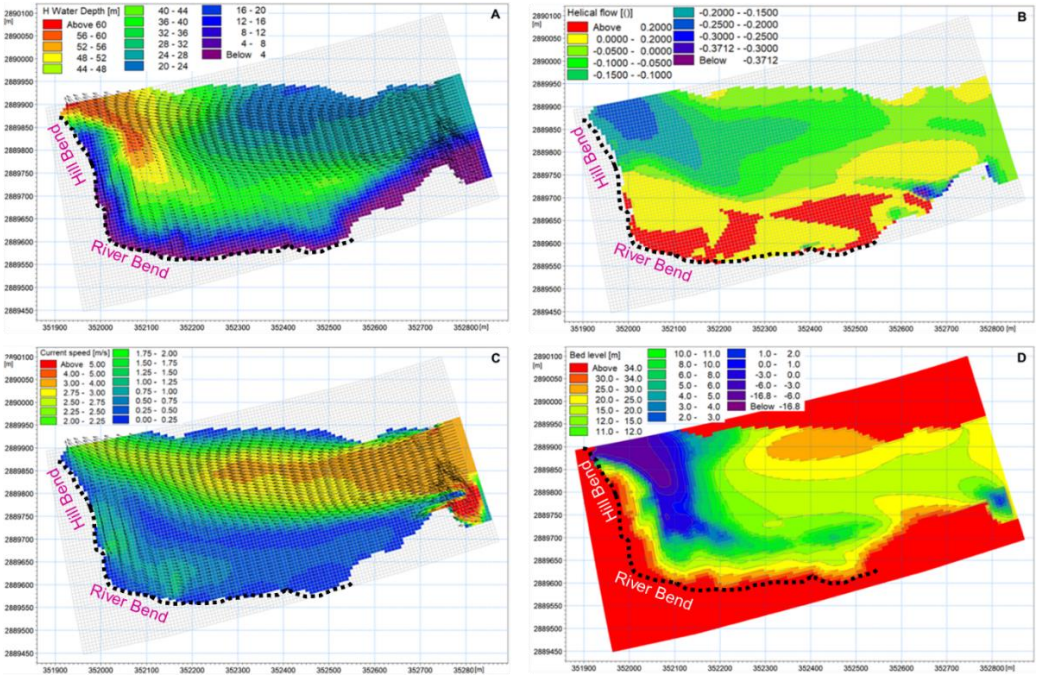


Figure 5. (A) spatial distribution of depth-averaged primary flow, (B) patterns of dimensionless helical flow intensity (secondary flow structure), (C) velocity magnitude (current speed), and (D) longitudinal variation in bed elevation along the hill-bend study reach near Palasbari town.

Table 4. Summary of measured data and simulated hydraulic parameters along the south bank of the study reach, and Pandu gauging station.

Hydraulic variables		Measured data	Simulated	
			1 in 2-year flood (bankfull discharge)	1 in 100-year flood
Pandu gauging station				
Depth (m)	Maximum		63.23	65.24
	Average		28.64	29.32
Water level (m, amsl)	Maximum		47.35	49.52
	Average	47.23	47.25	49.27
	Minimum		47.06	48.67
Speed (m/s)	Maximum		02.97	04.83
	Average		01.24	02.05
Study reach		Yr-2024		
Discharge (m^3/s)	Average		10,073	16,943
Depth (m)	Maximum	33.03	33.83	35.49
	Average	09.05	09.84	11.48
Water level (m, amsl)	Maximum	46.88	47.72	49.59
	Average	46.42	47.13	48.85
	Minimum	46.04	46.73	48.23
Speed (m/s)	Maximum	02.51	02.81	03.31
	Average	01.23	01.43	01.83

4.4.2. Model calibration

Hydraulic calibration: Hydraulic calibration involves adjusting flow resistance parameters to ensure the modelled water levels align with observed data. In this study, Manning's resistance formulation was adopted, with the calibration performed iteratively using the model in hydrodynamic-only mode (i.e., excluding river morphological processes). The Manning's roughness coefficient (expressed as Manning's M) was systematically varied to optimize the agreement with observed upstream water levels (Figure 6).

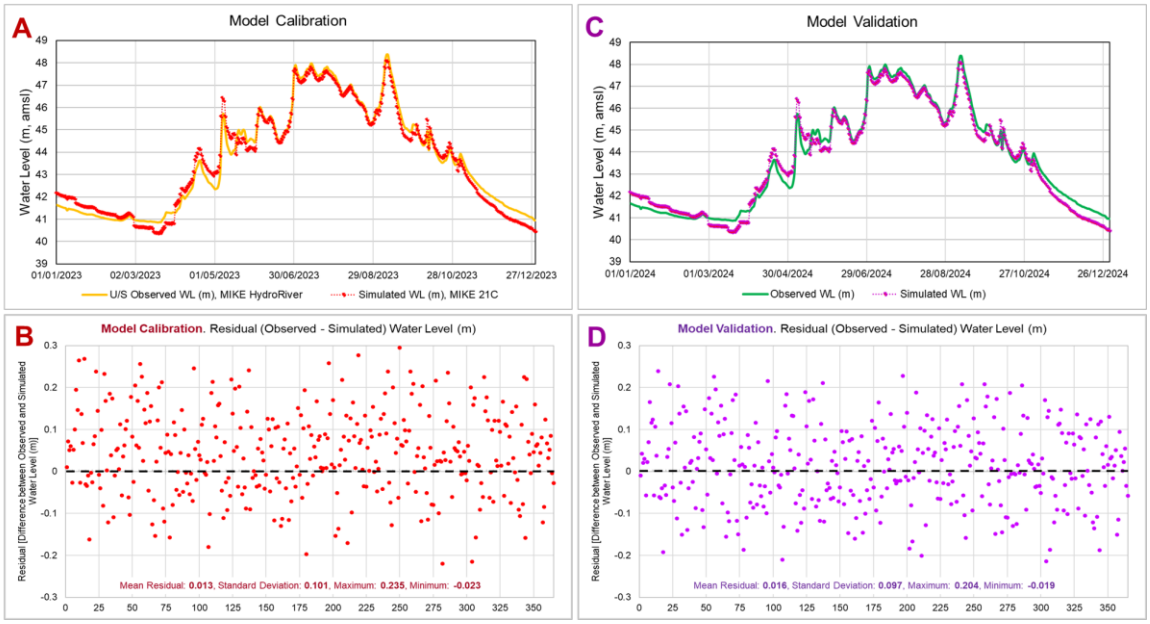


Figure 6. (A) Calibration of water levels for hydraulic resistance estimation; (B) residual analysis of the calibrated model; (C) validation of simulated water levels; (D) residual analysis of the validated model.

The calibration yielded Manning's M values ranging from 22 to 35, while calibration yielded a Manning's M value of 23 $m^{1/3}/s$, indicative of relatively high flow resistance-consistent with conditions typical of large, vegetated, and weed-infested rivers. Although this value may appear high, further assessment confirmed its plausibility within the context of the site-specific hydraulic characteristics. Water levels were carefully calibrated and subsequently validated, demonstrating excellent agreement with observed data. In addition, residual error analysis was performed for both calibration and validation phases, revealing minimal bias and confirming a strong model fit across the entire simulation period.

Figure 6 provides a comprehensive assessment of the hydrodynamic model's performance through calibration and validation analyses, presented in four panels. The panel (A) depicts the calibration phase for 2023, where observed upstream water levels (U/S observed WL) obtained from MIKE Hydro River are compared against simulated water levels generated by MIKE 21C. This comparison demonstrates the model's ability to reproduce temporal variations in water levels under observed flow conditions. The panel (C) presents the validation phase for 2024, contrasting observed water levels with MIKE 21C simulations to evaluate the model's predictive capability under independent datasets. The panel (B) shows the residuals (observed - simulated) during calibration, providing a quantitative measure of model accuracy. The residual distribution indicates a mean bias of 0.013 m, with variability characterized by a standard deviation of 0.101 m and extremes ranging between -0.023 m and 0.235 m. The panel (D) displays the residuals during validation, with a mean bias of 0.016 m, a standard deviation of 0.097 m, and values spanning -0.019 m to 0.204 m. Collectively, these panels demonstrate that the model achieves close agreement with observed water levels, with residuals remaining within acceptable limits for hydrodynamic simulations. The integrated presentation of calibration and validation results, alongside residual statistics, provides a coherent evaluation of

model robustness, accuracy, and reliability across different temporal datasets.

It is important to note that the model demonstrates superior performance under high discharges conditions, whereas it tends to overestimate water levels during low-flow (dry season) periods relative to MIKE Hydro River outputs. Such deviations between high and low discharge calibrations are frequently observed in hydrodynamic modeling.

In morphodynamic applications, minor discrepancies during low-flow periods are generally considered acceptable due to the nonlinear nature of sediment transport processes, which are predominantly driven by high-flow events.

Sediment transport calibration: Following the calibration of hydraulic resistance, the sediment transport component was subsequently adjusted. This was performed with the sediment transport module activated alongside bathymetric updating, enabling dynamic feedback between sediment movement and bed level changes.

The Engelund-Hansen total load transport formula [94] was adopted for simulating sediment dynamics in the study reach. To align model output with the observed sediment rating curve, a scaling factor of 0.4 was applied to the original formulation. This modification is considered justifiable, as it remains within a reasonable range near unity and ensures that the sediment transport estimates remain physically realistic (Figure 7). In contrast, applying a substantially lower factor, such as 0.01, would undermine the empirical integrity of the model and compromise its realism. The observed sediment rating curve used for calibration was derived from sediment flux data reported at the Pandu gauging station, using both available field measurements and values from established literature.

Since the Engelund-Hansen equation provides an estimate of the total sediment load, a load partitioning scheme was applied in order to distinguish between suspended and bed material transport. In this study, 75% of the total load was assigned to the suspended fraction. This choice is supported by sedimentological investigations of the Brahmaputra River and other large alluvial rivers, which consistently highlight the dominance of suspended material in the transport regime, particularly during monsoonal high flows. Previous field observations and sediment rating analyses (e.g. [23, 89]) indicate that suspended load typically constitutes 70-90% of the total sediment flux, with the remainder comprising bed load. Adopting 75% as the suspended fraction therefore lies well within the empirically observed range and aligns with established morphodynamic modeling practices for large sand-bed rivers. This approach not only reflects the natural transport dynamics of the Brahmaputra but also provides a stable and physically realistic input for the model simulations.

The application of the Engelund-Hansen sediment transport formula, though widely accepted, involves empirical adjustments that introduce uncertainty. The use of a 0.4 scaling factor, while within a reasonable range, reflects model calibration to observe data at the Pandu gauging station and may not fully capture temporal variability or extreme flow conditions. Additionally, the assumed 75% suspended load partitioning, although appropriate for large rivers like Brahmaputra, does not account for spatial heterogeneity in flow and sediment dynamics. Limited grain size and bathymetric data also contribute to uncertainty in hydraulic roughness and sediment flux estimation. These factors underscore the need for continuous field data and probabilistic approaches to improve model robustness and reduce uncertainty.

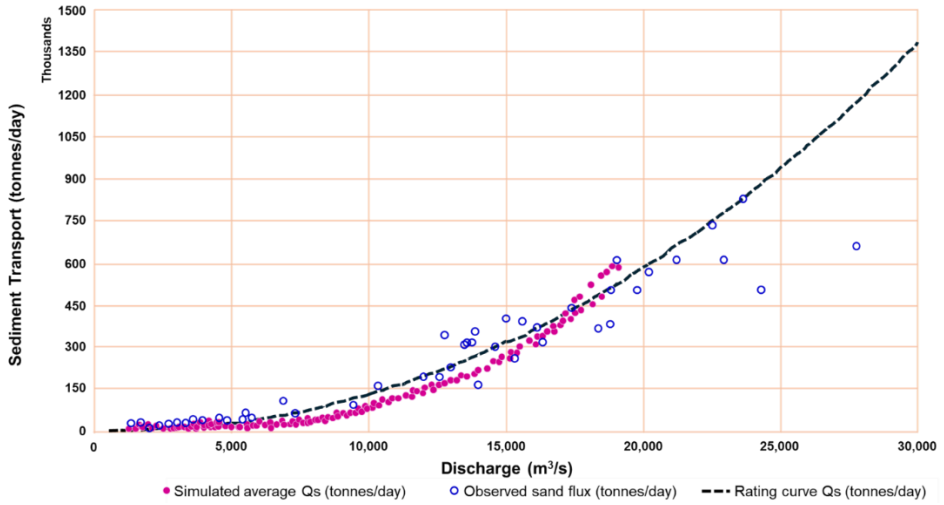


Figure 7. Sediment transport model calibration.

The sediment transport model was rigorously calibrated and validated using observed sediment data expressed in tonnes per day. The calibration process involved adjusting model parameters to match the temporal variations of observed sediment flux, while the validation confirmed the model's ability to reliably reproduce sediment transport dynamics within the study reach. This approach ensures that the simulated sediment flux captures both the magnitude and temporal patterns of sediment transport under varying flow conditions. Figure 8 subsequently illustrates the comparison between observed and simulated sediment flux values, demonstrating the model's performance.

The sediment transport model was successfully calibrated and validated using observed data expressed in tonnes per day (Figure 8). The simulated results closely matched the observed sediment transport values in both phases, demonstrating the robustness of the model. Residual analysis was also conducted for calibration and validation, which showed minimal errors and no significant bias, indicating a strong agreement between observed and simulated values and confirming the reliability of the model's performance.

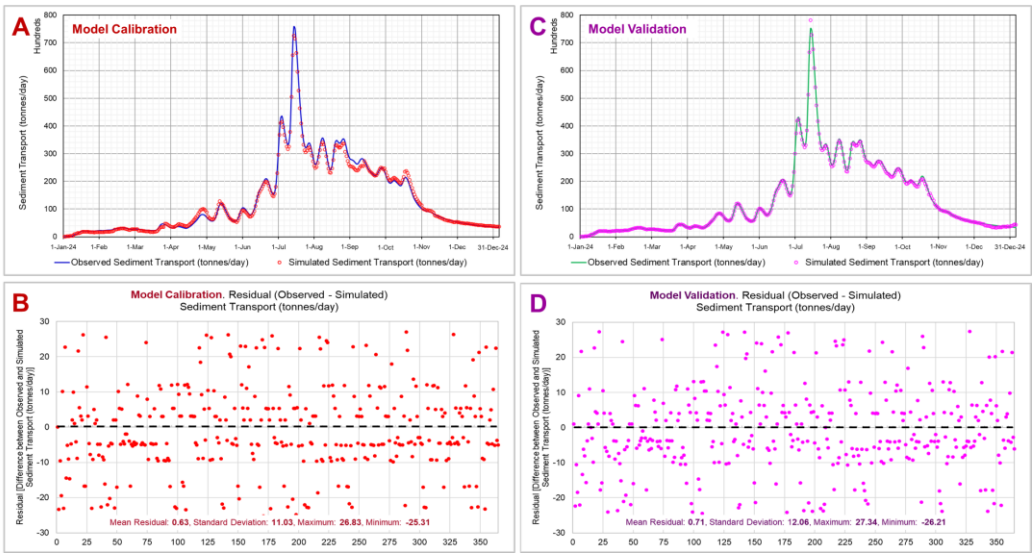


Figure 8. (A) Calibration of sediment transport; (B) residual analysis of the calibrated model; (C) validation of simulated sediment transport; (D) residual analysis of the validated model.

Figure 8 presents a comprehensive evaluation of the sediment transport model performance through calibration and validation analyses, organized into four panels. The top-left panel (A) shows the calibration phase, where observed sediment transport (tones/day) is compared against simulated values from January to December 2023. This time-series comparison highlights the model's ability to reproduce seasonal variability and peak transport events, particularly during the monsoon period. The bottom-left panel (B) displays the residuals (observed - simulated) for the calibration dataset, providing a quantitative measure of model accuracy. The residual distribution indicates a mean bias of 0.63 tonnes/day, with variability characterized by a standard deviation of 11.03 tonnes/day and extremes ranging between -25.31 and 26.83 tonnes/day.

The top-right panel (C) represents the validation phase, where observed sediment transport data from an independent dataset (January-December 2024) are compared with simulated values. This panel demonstrates the model's predictive capability under conditions not used for calibration. The bottom-right panel (D) shows the residuals for the validation dataset, with a mean bias of 0.71 tonnes/day, a standard deviation of 12.06 tonnes/day, and values spanning -26.21 to 27.34 tonnes/day. Collectively, these four panels provide an integrated assessment of model performance, demonstrating that the calibration and validation procedures were conducted using distinct temporal datasets, and that the residuals remain within acceptable limits for sediment transport simulations.

5. Results and discussion

5.1. Approaches to mitigate erosion risks

The study reach bend has exhibited significant morphological activity since 2024. Historical bankline analysis from 2013 to 2024 indicates that the reach remained relatively stable until recent years. However, post-2024 observations reveal substantial bank erosion and bend migration, resulting in the formation of deep scours and incised channels, with general scour depths ranging from 20 to 30 meters-local scour depths being considerably greater. This heightened morphological sensitivity, particularly in the context of ongoing and future developmental activities, necessitates a carefully engineered approach to erosion mitigation. Any proposed intervention must account for potential risks such as continued scour progression, compromised structural stability of the hill adjacent to the study reach, accelerated bank retreat, and long-term threats of bend evolution and out-flanking.

To evaluate these concerns, two mitigation scenarios were tested using hydrodynamic modeling under a 1-in-100-year flood condition [95]. The objective was not only to identify favourable effects but also to assess potential negative consequences, thereby informing risk-aware decision-making. It is strongly advised that all proposed mitigation strategies be subjected to rigorous scenario-based modeling and risk assessment prior to implementation. While current simulations were limited to hydrodynamic analyses, a more robust evaluation would require morphological modeling over extended temporal scales. This necessitates high-resolution bathymetric data and model domain expansion to reduce uncertainty associated with boundary condition influences. The constrained spatial extent of the current model introduces limitations for long-term morphological predictions, underscoring the need for more comprehensive data and modeling frameworks in future assessments.

5.2. Charland dredging and bend spoil disposal

Dredging is planned in the shallow charland located on the opposite side of the eroding

bank. In the model, approximately 8 meters of material is removed through dredging, and the excavated sediment is subsequently deposited along the eroded bank, forming a raised feature approximately 10 meters high (Figure 9). The primary objective of this intervention is to redirect the primary flow into the newly dredged channel, thereby reducing flow impingement on the outer bank. Concurrently, the strategic placement of dredged material at the eroded bend is intended to diminish local flow circulation and suppress the formation of secondary currents-mechanisms that are often responsible for enhancing bend scour and accelerating bank erosion. This approach, simulated under conditions equivalent to a 2-year return period flood, aims to stabilize the bend and mitigate further morphological degradation.

5.3. Assessment of flow deflection

The proposed flow deflection structures upstream are intended to achieve objectives similar to those of dredging the shallow charland located opposite the bank. These structures are designed to redirect the main flow toward the opposite side, thereby enhancing scouring and improving channel conveyance (Figure 10). The simulations for these structures were performed under conditions equivalent to a 2-year return period flood. However, their implementation is also being assessed for potential adverse impacts. Given that the study reach is a short and dynamically evolving meander bend, it is critical to evaluate whether the introduction of such deflection structures induces increased eddy formation or intensified secondary currents immediately downstream conditions that may be more detrimental than the existing hydraulic and morphological state.

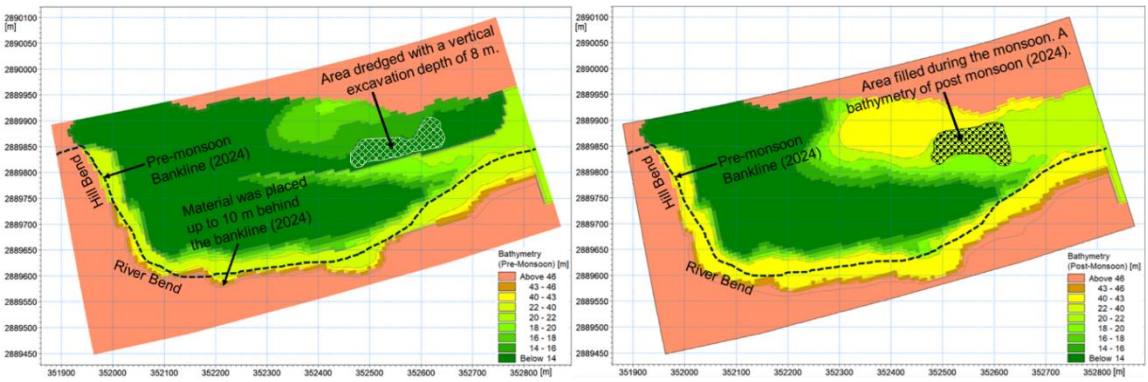


Figure 9. Dredging and material disposal scenarios are illustrated for the pre-monsoon (left) and post-monsoon (right) periods of 2024.

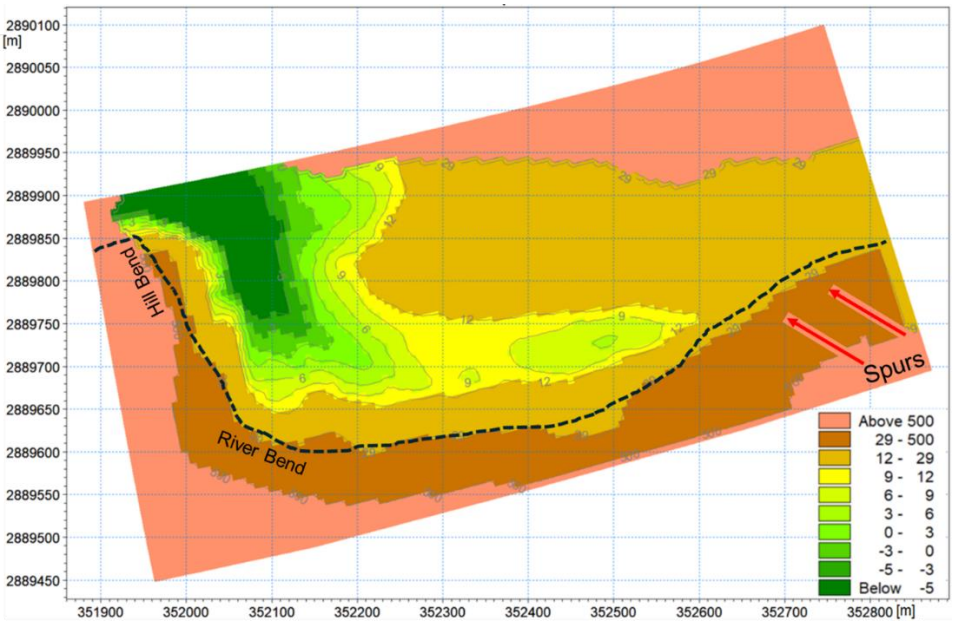


Figure 10. Spur structures designed to alter flow direction are situated roughly 1 km upstream from the hill segment of the study reach near Palasbari town.

5.4. Evaluation of dredging and sediment disposal scenario

The dredging and disposal scenario appears to be hydraulically favourable, as it reduces the intensity of flow circulation and facilitates increased discharge through the dredged channel section. In contrast, the flow deflection scenario-based solely on hydrodynamic simulations-demonstrates unfavourable outcomes. The deflected flow induces a bend-like circulation pattern toward the opposite charland, as clearly illustrated in Figure 11. This newly formed secondary flow pattern generates a pronounced reverse current along the bank situated behind the hill, thereby intensifying local bank erosion. Consequently, any implementation of flow deflection measures, even if positioned further upstream, must be approached with caution and underpinned by detailed morphological and hydraulic assessments.

It is also important to note that the hill bend within the study reach exhibited relative morphological stability during the period from 2021 to 2024. However, significant morphological activity has been observed post-2024. This raises the need for a thorough investigation into whether any upstream flow interventions may have contributed to this recent instability.

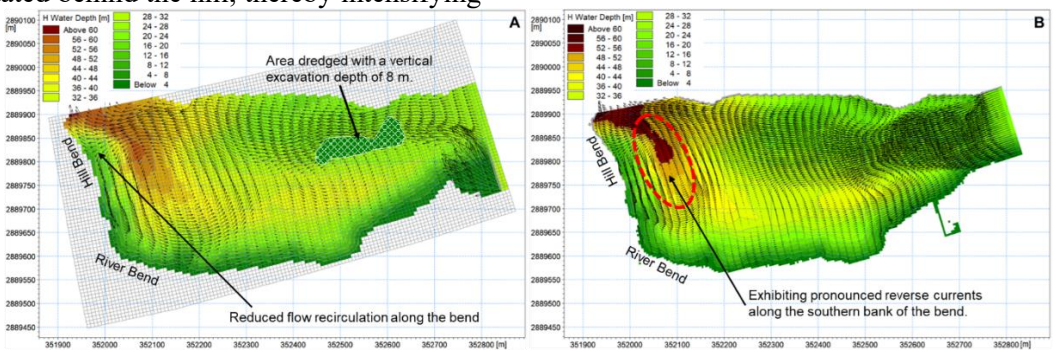


Figure 11. (A) Hydrodynamic simulation of dredging and dumping under a 100-year flood event, showing reduced flow recirculation along the bend; (B) Flow deflection scenario, illustrating increased circulation toward the opposite charland with stronger reverse currents along the southern bank bend.

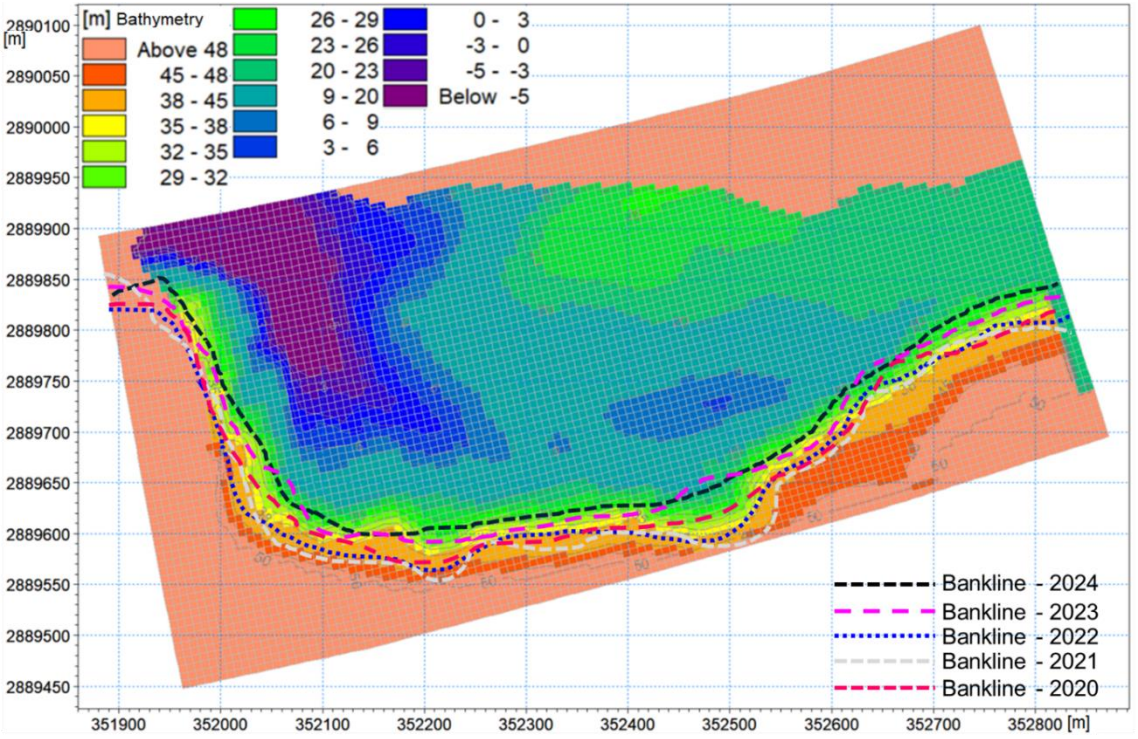


Figure 12. Bathymetric data from the post-monsoon 2024, along with bankline migration observed between 2020 and 2024.

Figure 11 compares two hydrodynamic scenarios under a 100-year flood event. In Panel A, the dredging and dumping scenario reduces flow recirculation along the bend. This outcome is evident from the velocity and depth patterns, which show smoother flow alignment and diminished reverse currents. Such reduction in recirculation can potentially stabilize the bend by lowering localized turbulence and minimizing sediment deposition.

In Panel B, the flow deflection scenario produces the opposite effect. The simulations indicate increased circulation, with the main current curving toward the opposite charland. This deflected flow generates stronger reverse currents along the southern bank bend. The intensified recirculation enhances shear stress on the bank, which may exacerbate erosion processes. The comparison between the two panels highlights how different intervention strategies can either mitigate or amplify bend instability, underscoring the importance of scenario-based hydrodynamic analysis in river management.

Once an erosion protection revetment-such as those constructed using geo-bags or cement concrete blocks installed along an erosion-prone reach of the Brahmaputra River, two outcomes are typically observed: (i) the structure remains functional with the main flow aligned along the protected bank, or (ii) the primary flow path migrates away from the structure, rendering it ineffective or abandoned. Both scenarios have been documented in various reaches of the Brahmaputra. In the first case, where the revetment remains functional and the main flow continues to run adjacent to the protected bank, one consistent hydraulic response is observed: increased bank erosion and bed scour immediately downstream of the revetment. This is attributed to the fact that the protected section resists erosion, thereby causing the flow-now sediment-deprived or 'hungry'-to aggressively erode the downstream unprotected bank and bed. Such a phenomenon has been observed at the hill bend within the current study reach. Satellite-derived bankline analyses (Figure

12) indicate that this bend remained relatively stable from 2020 to 2024. However, under present conditions, the reach is experiencing significant bank erosion and bed degradation. Predictive simulations using the local 2D hydrodynamic model suggest that this erosion trend will persist, with further bed scour anticipated, particularly near the toe of the hill within the study reach. These developments present several potential future risks and management implications that warrant detailed investigation.

5.5. Future morphological risk and flow realignment strategy

In the context of ongoing bank erosion, it is imperative to consider potential future risks-particularly the possibility of the river outflanking the study reach hill and rejoining the main flow channel immediately downstream. This scenario, while extreme, cannot be categorically ruled out. Regardless of whether such a course shift occurs, maintenance interventions are likely to be undertaken to mitigate the current bank erosion. However, once lateral bank migration is arrested through such protective measures, the ongoing bed scour at the toe of the hill has already reached considerable depths expected to intensify. Predictions from the local 2D hydrodynamic model indicate continued deepening of this scour zone. It is important to note that the hill at the study reach is currently functioning in a manner analogous to an engineered spur. Typically, spurs are designed with sloped aprons and the placement of scour-resistant material along the riverbed to counteract localized erosion. In contrast, the study reach hill lacks such protective features, making it particularly vulnerable to undermining by continued scour. This condition poses a significant threat to the structural and geotechnical stability of the hill under the 100-year return period.

As a potential solution to mitigate further scour, it is essential not only to protect the eroding bank but also to divert the main flow away from the bank and the study reach hill. This flow realignment should be initiated upstream of the current model domain, preferably through strategic dredging of a new channel across the opposite charland to guide the discharge away from the vulnerable bankline. While flow deflection using structural measures such as spurs or groynes may also be considered, their placement must be carefully evaluated. Specifically, such structures should not be positioned in the immediate upstream vicinity of the study reach hill. Results from the 2D hydrodynamic model demonstrate that introducing a deflector approximately 1 km upstream of the hill could produce adverse hydraulic effects, including intensified bank erosion. Therefore, the optimal location and design of any deflector must be assessed within an expanded modelling framework that captures a larger spatial domain and integrates both morphological and hydraulic considerations.

6. Conclusions

This study employs a high-resolution 2D hydrodynamic and morphodynamic modeling framework (MIKE 21C) to evaluate erosion risk and inform hydraulic design for a dynamically migrating meander bend along the Brahmaputra River—one of the world's most sediment-laden and hydrologically dynamic alluvial systems. By Simulating two critical hydrological scenarios-the 2-year bankfull discharge and the 1-in-100-year flood—the study provides new insights into extreme morphological responses and sediment dynamics under high-flow conditions. The findings include peak velocities of 4.83 m/s and flow depths exceeding 65 m, and water levels reaching 49.92 m amsl near the Pandu station. The southern bank behind the hill emerged as a persistent high-energy zone, where secondary currents and localized reverse flows (>2 m/s) contributed to progressive bank retreat and deep local scour (>30 m), clearly exceeding sediment motion threshold for 0.24 mm sand, confirming that

the reach is highly susceptible to erosion during frequent flood events.

This work advances current scientific understanding by integrating site-specific sediment calibration (Manning's M of 23 $m^{1/3}/s$; Engelund–Hansen total load formula with 0.4 scaling and 75% suspended load) with scenario-based intervention testing —an approach rarely applied with such spatial and hydraulic detail in the Brahmaputra context. Two mitigation strategies were evaluated under extreme flood conditions: (i) dredging the shallow charland opposite the eroding bank and depositing excavated sediment along the outer bend, and (ii) installing upstream flow deflectors. The dredging-disposal scenario approach reduced erosive flow patterns, while deflectors intensified reverse flow and erosion, underscoring the potential for misinformed structural interventions to exacerbate degradation.

The study also fills a critical research gap by documenting post-2024 bed and bank instability —following a decade of morphological stability—linking it to possible upstream changes and highlighting the urgency for adaptive, system-scale river management. The findings advocate for sediment-guided flow realignment over hard engineering, reinforcing the necessity of domain-wide, process-based morphological modeling to inform sustainable and technically sound riverbank protection in complex alluvial environments.

7. Recommendations

Based on the findings of this study, a set of technical and management-oriented recommendations is proposed to mitigate bank erosion and morphological instability in the dynamic reach of the Brahmaputra River near Palasbari. First, dredging the mid-channel bar (charland) opposite the eroding bank and strategically placing the excavated material along the outer bend proved to be an effective intervention. This approach minimized secondary circulation and high-energy zones along the vulnerable bankline, thereby reducing erosion risk. It is recommended that such sediment-guided realignment strategies be prioritized over hard-engineering structures in similar settings.

Second, structural interventions such as flow deflectors or groynes should not be implemented without extensive hydraulic and morphological simulation. Model results indicate that improper placement—especially near or upstream of the study reach hill—can exacerbate reverse flow and erosion. Any deflector must be positioned with caution and should be evaluated within an extended domain that captures upstream flow conditions, sediment dynamics, and potential feedback mechanisms.

Third, immediate action is needed to stabilize the hill toe, which is currently subject to deepening scour. This may involve the installation of a sloped scour apron using geobags or concrete mattresses to resist undermining forces. Long-term protection measures must integrate both bank stabilization and bed protection strategies.

Fourth, the recent morphological instability observed after 2024 underscores the influence of upstream changes. Therefore, a system-scale monitoring program should be implemented, incorporating satellite-based bankline tracking, bathymetric surveys, and sediment load monitoring to assess cumulative impacts.

Finally, future river training projects should adopt a process-based modeling approach like MIKE 21C to design adaptive and scientifically validated solutions. This ensures that interventions are not only locally effective but also system-compatible, preserving the morphological and hydraulic integrity of one of the world's most complex alluvial rivers. Future studies could also focus on evaluating the optimal frequency of sediment-guided interventions, considering the evolving morphology of the river reach. Moreover, comprehensive assessments of the economic feasibility, technical requirements, and long-term sustainability of such strategies would

provide valuable guidance for practical implementation in similar dynamic riverine environments.

Acknowledgment

Authors are grateful to Managing Director, DHI (India) Water & Environment Pvt Ltd, New Delhi, India for providing the necessary facilities to carry out this work.

Declarations

Ethical Approval: This study did not involve any human participants or animal subjects, and therefore ethical approval was not required.

Consent to Participate: Not applicable. This study did not involve human participants, and therefore no consent to participate was required.

Consent to Publish: Not applicable. This study does not include any individual data or images requiring consent for publication.

Data Availability Statement: The links to publicly available datasets used in this study are provided in the data used section. Other datasets that were collected and analyzed during the study are available from the corresponding author upon reasonable request.

Clinical Trial Number: Not applicable.

Funding Statement: This research was conducted without any external funding.

Conflict of Interest: The authors declare that there are no conflicts of interest regarding the publication of this manuscript.

AI Statement: The authors did not use any artificial intelligence (AI) tools or services in the preparation of this work.

Author Contributions: KP conceptualized and formulated the research study. KP was responsible for the acquisition and analysis of the dataset. UP provided valuable assistance in the hydrological modeling aspects of the study. KP and UP both contributed to the interpretation of the research findings. KP prepared the initial manuscript draft. The final version of the manuscript was critically reviewed, revised, and approved by KP and UP.

References

1. Church M. Channel stability: morphodynamics and the morphology of rivers. In: Rowiński P, Radecki-Pawlik A, editors. *Rivers – physical, fluvial and environmental processes*. GeoPlanet: Earth and Planetary Sciences. Cham: Springer; 2015. https://doi.org/10.1007/978-3-319-17719-9_12
2. Lightbody AF, Kui L, Stella JC, Skorko KW, Bywater-Reyes S, Wilcox AC. Riparian vegetation and sediment supply regulate the morphodynamic response of an experimental stream to floods. Front Environ Sci. 2019;7:40. https://doi.org/10.3389/fenvs.2019.00040
3. Nittrouer JA, Shaw J, Lamb MP, Mohrig D. Spatial and temporal trends for water-flow velocity and bed-material sediment transport in the lower Mississippi River. GSA Bull. 2012;124(3-4):400–414. https://doi.org/10.1130/B30497.1
4. Hooke J. Morphodynamics of active meandering rivers reviewed in a hierarchy of spatial and temporal scales. Geomorphology. 2023;439. https://doi.org/10.1016/j.geomorph.2023.108825
5. Thomas R, Nicholas A. Simulation of braided river flow using a new cellular routing scheme. Geomorphology. 2002;43:179–195. https://doi.org/10.1016/s0169-555x(01)00128-3
6. Kasprak A, Brasington J, Hafen K, Williams RD, Wheaton JM. Modelling braided river morphodynamics using a particle travel length framework. Earth Surf Dyn. 2019;7:247–274. https://doi.org/10.5194/esurf-7-247-2019
7. Kulnu AS, Hazarika N, Bharali P. Evolution and morphodynamics of the large-braided river Brahmaputra during the last four decades of the Quaternary epoch: a spatio-temporal assessment using geoinformatics. Int J River Basin Manag. 2024:1–19. https://doi.org/10.1080/15715124.2024.2421372
8. Church M, Ferguson RI. Morphodynamics: rivers beyond steady state. Water Resour Res. 2015;51(4):1883–1897. https://doi.org/10.1002/2014WR016862
9. Hohensinner S, Hauer C, Muhar S. River morphology, channelization, and habitat restoration. In: Schmutz S, Sendzimir J, editors. *Riverine ecosystem management*. Aquatic Ecology Series. Vol. 8. Cham: Springer; 2018. https://doi.org/10.1007/978-3-319-73250-3_3
10. Schuurman F, Marra WA, Kleinhans MG.

Physics-based modeling of large-braided sand-bed rivers: bar pattern formation, dynamics, and sensitivity. J Geophys Res Earth Surf. 2013;118(4):2509–2527. https://doi.org/10.1002/2013JF002896
11. Williams RD, Brasington J, Hicks DM. Numerical modelling of braided river morphodynamics: review and future challenges. Geogr Compass. 2016;10(3):102–127. https://doi.org/10.1111/gec3.12260
12. Hicks DM, Baynes ERC, Measures R, Stecca G, Tunnicliffe J, Friedrich H. Morphodynamic research challenges for braided river environments: lessons from the iconic case of New Zealand. Earth Surf Process Landf. 2021;46(1):188–204. https://doi.org/10.1002/esp.5014
13. Pareta K. Morphological study of Brahmaputra River in Assam based on historical Landsat satellite imagery from 1996 to 2020. Am J Environ Sustain Dev. 2021;6(2). http://www.aiscience.org/journal/paperInfo/ajesd?paperId=5293
14. Tubaldi E, White CJ, Patelli E, Mitoulis SA, de Almeida G, Brown J, Cranston M, Hardman M, Koursari E, Lamb R, McDonald H, Mathews R, Newell R, Pizarro A, Roca M, Zonta D. Invited perspectives: challenges and future directions in improving bridge flood resilience. Nat Hazards Earth Syst Sci. 2022;22:795–812. https://doi.org/10.5194/nhess-22-795-2022
15. Uddin MJ, Shakik A, Mim FB. Understanding the impact of bridge structure on river morphology through geospatial techniques: case on Teesta River, Bangladesh. Discover Environ. 2024;2:91. https://doi.org/10.1007/s44274-024-00136-z
16. Wright N, Crosato A. The hydrodynamics and morphodynamics of rivers. In: Wilderer P, editor. *Treatise on water science*. Vol. 2. Oxford: Academic Press; 2011. p.135–156. https://www.academia.edu/23806974/The_Hydrodynamics_and_Morphodynamics_of_Rivers
17. Ashmore P. Morphology and dynamics of braided rivers. In: Shroder J, Wohl E, editors. *Treatise on geomorphology*. Vol. 9: fluvial geomorphology. San Diego: Academic Press; 2013. p.289–312. https://doi.org/10.1016/B978-0-12-374739-6.00242-6
18. Eke E, Parker G, Shimizu Y. Numerical modeling of erosional and depositional bank processes in migrating river bends with self-formed width: morphodynamics of bar push and bank pull. J Geophys Res Earth Surf. 2014;119(7):1455–1483. https://doi.org/10.1002/2013JF003020
19. Chadwick AJ, Steel E, Passalacqua P, Paola C. Differential bank migration limits the lifespan and width of braided channel threads. Water Resour Res. 2022;58(8). https://doi.org/10.1029/2021WR031236
20. Wal MVD. Bank protection structures along the Brahmaputra-Jamuna River, a study of flow slides. Water. 2020;12(9). https://doi.org/10.3390/w12092588
21. Pareta K. River morphological modelling of Brahmaputra River, Assam. Int J Hydropower Civ Eng. 2021;2(2):8–17. https://www.civilengineeringjournals.com/ijhce/article/13/3-1-1-892.pdf
22. Debnath J, Sahariah D, Lahon D, Nath N, Chand K, Meraj G, Kumar P, Singh SK, Kanga S, Farooq M. Assessing the impacts of current and future changes of the planforms of river Brahmaputra on its land use-land cover. Geosci Front. 2023;14(4). https://doi.org/10.1016/j.gsf.2023.101557
23. Sarma JN. Fluvial process and morphology of the Brahmaputra River in Assam, India. Geomorphology. 2005;70(3-4):226–256. https://doi.org/10.1016/j.geomorph.2005.02.007
24. Gautam S, Singh A, Dhanya CT, Chandrika. Increased socio-economic vulnerability in the floodplains of Brahmaputra Basin, India. vEGU21, the 23rd EGU General Assembly. 2021. https://meetingorganizer.copernicus.org/EGU21/EGU21-3193.html
25. Pareta K. River morphology of braided Brahmaputra River, Assam, India. Chisinau: LAP Lambert Academic Publishing, Republic of Moldova; 2022. p.1–444. https://www.morebooks.shop/shop-ui/shop/book-launch-offer/1471e9b08e1f2677f4f2c18a12d1dbe6e60d2cdc
26. Sarker S, Sarker T, Leta OT, Raihan SU, Ahmed N. Understanding the planform complexity and morphodynamic properties of Brahmaputra River in Bangladesh: protection and exploitation of riparian areas. Water. 2023;15(7):1384. https://doi.org/10.3390/w15071384
27. Summer S, Walling DE. Modelling erosion, sediment transport and sediment yield. IHP-VI Technical Documents in Hydrology No.

60. Paris: UNESCO; 2002. https://www.hydrology.nl/images/docs/ihp/2002_Modelling_erosion_sediment_127848e.pdf
28. Pareta K, Jakobsen F, Joshi M. Morphological characteristics and vulnerability assessment of Alaknanda, Bhagirathi, Mandakini and Kali rivers, Uttarakhand (India). Am J Geophys Geochem Geosyst. 2019;5(2):49–68. http://www.aiscience.org/journal/paperInfo/aj3g?paperId=4645
29. Mir AA, Patel M. A comprehensive review on sediment transport, flow dynamics, and hazards in steep channels. J Water Manag Model. 2024. https://doi.org/10.14796/JWMM.C517
30. Andualem TG, Hewa GA, Myers BR, Peters S, Boland J. Erosion and sediment transport modeling: a systematic review. Land. 2023;12(7):1396. https://doi.org/10.3390/land12071396
31. Hu Y, Yang H, Zhou H, Lv Q. A review of numerical modelling of morphodynamics in braided rivers: mechanisms, insights and challenges. Water. 2023;15(3):595. https://doi.org/10.3390/w15030595
32. Pareta K. 1D-2D hydrodynamic and sediment transport modelling using MIKE models. Discover Water. 2024;4:94. https://doi.org/10.1007/s43832-024-00130-9
33. Brown RA. Hydrogeomorphic scaling and ecohydraulics for designing rescaled channel and floodplain geometry in regulated gravel–cobble bed rivers for Pacific salmon habitat. Water. 2022;14(4):670. https://doi.org/10.3390/w14040670
34. Odey G, Cho Y. Event-based vs. continuous hydrological modeling with HEC-HMS: a review of use cases, methodologies, and performance metrics. Hydrology. 2025;12(2):39. https://doi.org/10.3390/hydrology12020039
35. Darby S, Sear D. River restoration: managing the uncertainty in restoring physical habitat. Hoboken: John Wiley & Sons Inc.; 2008. https://www.academia.edu/Documents/in/River_Restoration?swp=tc-ri-1156513
36. Javernick L, Hicks DM, Measures R, Caruso B, Brasington J. Numerical modelling of braided rivers with structure-from-motion-derived terrain models. River Res Appl. 2015;32(5):1071–1081. https://doi.org/10.1002/rra.2918
37. Kasvi E, Alho P, Lotsari E, Wang Y, Kukko A, Hyyppä H, Hyyppä J. Two-dimensional and three-dimensional computational models in hydrodynamic and morphodynamic reconstructions of a river bend: sensitivity and functionality. Hydrol Process. 2014;29(6):1604–1629. https://doi.org/10.1002/hyp.10277
38. Horvat Z, Isic M, Spasojevic M. Two-dimensional river flow and sediment transport model. Environ Fluid Mech. 2015;15:595–625. https://doi.org/10.1007/s10652-014-9375-y
39. Zhang Y, Al-Hamdan M, Wren D. Development of a two-dimensional hybrid sediment-transport model. Appl Sci. 2023;13(8):4940. https://doi.org/10.3390/app13084940
40. Lai YG, Thomas RE, Ozeren Y, Simon A, Greimann BP, Wu K. Modeling of multilayer cohesive bank erosion with a coupled bank stability and mobile-bed model. Geomorphology. 2015;243:116–129. https://doi.org/10.1016/j.geomorph.2014.07.017
41. Lai YG. Modeling stream bank erosion: practical stream results and future needs. Water. 2017;9(12):950. https://doi.org/10.3390/w9120950
42. Dubuis R, Cesare GD. The clogging of riverbeds: a review of the physical processes. Earth-Science Reviews. 2023;239. https://doi.org/10.1016/j.earscirev.2023.104374
43. Morianou GG, Kourgialas NN, Karatzas GP, Nikolaidis NP. Hydraulic and sediment transport simulation of Koiliaris River using the MIKE 21C model. Procedia Engineering. 2016;162C:463–470. https://doi.org/10.1016/j.proeng.2016.11.089
44. Vozinaki AEK, Morianou GG, Alexakis DD, Tsanis IK. Comparing 1D and combined 1D/2D hydraulic simulations using high-resolution topographic data: a case study of the Koiliaris basin, Greece. Hydrol Sci J. 2016;62(4):642–656. https://doi.org/10.1080/02626667.2016.1255746
45. DHI. MIKE 21C curvilinear model – scientific documentation. Horsholm: Danish Hydraulic Institute; 2022. https://manuals.mikepoweredbydhi.help/latest/Water_Resources/MIKE21C_Scientific_documentation.pdf
46. Ackers P, White WR. Sediment transport – new approach and analysis. J Hydraul Div. 1973;99(11):2041–2060.

https://ascelibrary.org/doi/10.1061/JYCEAJ.0003791
47. Borden C, Gaur A, Singh CR. Water resource software: application overview and review. Washington (DC): World Bank; 2016. https://documents1.worldbank.org/curated/en/279391467995445292/pdf/106396-WP-PUBLIC-WRS-SAWI-reportjune8.pdf
48. Enggrob HG, Tjerry S. Simulation of morphological characteristics of a braided river. In: River, Coastal and Estuarine Morphodynamics (RCEM) Proceedings; 1998. https://www.dhigroup.com/upload/publications/mike21/Vested_2014.pdf
49. Vested HJ, Tjerry S, Christensen BB, Dubinski IM. Numerical simulation of estuarine and river morphology. In: International Conference on Small Scale Morphological Evolution of Coastal, Estuarine and River Systems; Nantes; 2014.
50. Zongo J, Zabsonre JDD, Roamba B. Formal derivation of a new sediment transport model using a multiscale procedure: numerical validation. Partial Differ Equ Appl Math. 2024;9. https://doi.org/10.1016/j.padiff.2023.100606
51. Aksoy H, Mahe G, Meddi M. Modeling and practice of erosion and sediment transport under change. Water. 2019.
52. Sarker S. Essence of MIKE 21C (FDM numerical scheme): application on the river morphology of Bangladesh. Open J Model Simul. 2022;10:88–117. https://www.scirp.org/journal/paperinformation?paperid=116189
53. Pareta K. Morphological model for erosion prediction of India's largest braided river using MIKE 21C model. Earth Sci Syst Soc. 2024;4. https://doi.org/10.3389/esss.2024.10075
54. Ramakrishnan R, Rajawat AS. Simulation of suspended sediment transport initialized with satellite derived suspended sediment concentrations. J Earth Syst Sci. 2012;121:1201–1213. https://doi.org/10.1007/s12040-012-0222-6
55. Dang TA, Tran TH. Application of the MIKE21C model to simulate flow in the lower Mekong River basin. SpringerPlus. 2016;5:1982. https://doi.org/10.1186/s40064-016-3637-8
56. Karmaker T, Dutta S. Prediction of short-term morphological change in large braided river using 2D numerical model. J Hydraul Eng. 2016;142(10). https://doi.org/10.1061/(ASCE)HY.1943-7900.0001167
57. Morianou GG, Kourgialas NN, Karatzas GP, Nikolaidis NP. Assessing hydro-morphological changes in Mediterranean stream using curvilinear grid modeling approach – climate change impacts. Earth Sci Inform. 2018;11:205–216. https://doi.org/10.1007/s12145-017-0326-2
58. Wang Q, Peng W, Dong F, Liu X, Ou N. Simulating flow of an urban river course with complex cross sections based on the MIKE 21 FM model. Water. 2020;12(3):761. https://doi.org/10.3390/w12030761
59. Pareta K. Morphological dynamics of braided river near Bogibeel bridge, Assam. Int J Environ Plan Manag. 2021;7(3):72–86. https://www.semanticscholar.org/paper/Morphological-Dynamics-of-Braided-River-Near-Assam-Pareta/1e5ab6aecec070f531aef7da770f1abf2ac1507e
60. Le Xuan T, Nguyen Cong P, Vo Quoc T, Tran QQ, Wright DP, Anh DT. Multi-scale modelling for hydrodynamic and morphological changes of breakwater in coastal Mekong Delta in Vietnam. J Coast Conserv. 2022;26:18. https://doi.org/10.1007/s11852-022-00866-3
61. Sarker S. Separation of floodplain flow and bankfull discharge: application of 1D momentum equation solver and MIKE 21C. CivilEng. 2023;4(3):933–948. https://doi.org/10.3390/civileng4030050
62. Samir F. The impact of flow reduction on the river morphology during bridge rehabilitation. Ain Shams Eng J. 2025;16(5). https://doi.org/10.1016/j.asej.2025.103359
63. Jiang C, Parteli JR, Shao Y. A model for regional-scale water erosion and sediment transport and its application to the Yellow River Basin. J Adv Model Earth Syst. 2025;7(5). https://doi.org/10.1029/2024MS004593
64. Coleman JM. Brahmaputra river: channel processes and sedimentation. Sediment Geol. 1969;3(2–3):129–239. https://doi.org/10.1016/0037-0738(69)90010-4
65. Fischer S, Pietroń J, Bring A, Thorslund J, Jarsjö J. Present to future sediment transport of the Brahmaputra River: reducing uncertainty in predictions and management. Reg Environ Change. 2017;17:515–526. https://doi.org/10.1007/s10113-016-1039-7

66. Yannan J, Haining H. A new era for Tibet's rivers. Dialogue Earth. 2011. https://dialogue.earth/en/energy/4055-a-new-era-for-tibet-s-rivers/
67. Mahanta C, et al. Physical assessment of the Brahmaputra River. Dhaka: IUCN, International Union for Conservation of Nature; 2014. p.xii + 74. https://portals.iucn.org/library/sites/library/files/documents/2014-083.pdf
68. Samaranayake N, Limaye S, Wuthnow J. Water resource competition in the Brahmaputra River Basin: China, India and Bangladesh. CAN analysis and solution; 2016. https://www.cna.org/archive/CNA_Files/pdf/cna-brahmaputra-study-2016.pdf
69. Yasuda Y, Aich D, Hill D, Huntjens P, Swain A. Transboundary water cooperation over the Brahmaputra River: legal political economy analysis of current and future potential cooperation. The Hague: The Hague Institute for Global Justice; 2017. https://siwi.org/wp-content/uploads/2018/01/brahmaputra-basin-report-final_design.pdf
70. Palash W, Bajracharya SR, Shrestha AB, Wahid S, Hossain MS, Mogumder TK, Mazumder LC. Climate change impacts on the hydrology of the Brahmaputra River Basin. Climate. 2023;11(1):18. https://doi.org/10.3390/cli11010018
71. Mahanta C, Zaman AM, Newaz SMS, Rahman SMM, Mazumdar TK, Choudhury R, Borah PJ, Saikia L. Physical assessment of the Brahmaputra River: ecosystems for life, a Bangladesh-India initiative. Dhaka: IUCN, International Union for Conservation of Nature; 2014. https://portals.iucn.org/library/sites/library/files/documents/2014-083.pdf
72. Chauhan P, Singh N, Chauniyal DD, et al. Differential behaviour of a Lesser Himalayan watershed in extreme rainfall regimes. J Earth Syst Sci. 2017;126:22. https://doi.org/10.1007/s12040-017-0796-0
73. Rao MP, Cook ER, Cook BI, et al. Seven centuries of reconstructed Brahmaputra River discharge demonstrate underestimated high discharge and flood hazard frequency. Nat Commun. 2020;11:6017. https://doi.org/10.1038/s41467-020-19795-6
74. Vaithiyanathan P, Ramanathan AL, Subramanian V. Erosion, transport and deposition of sediments by the tropical rivers of India. In: Sediment budgets, proceedings of the Porto Alegre Symposium. IAHS Publ No. 174; 1988. https://iahs.info/uploads/dms/iahs_174_0561.pdf
75. Raff JL, Goodbred SL, Pickering JL, et al. Sediment delivery to sustain the Ganges-Brahmaputra delta under climate change and anthropogenic impacts. Nat Commun. 2023;14:2429. https://doi.org/10.1038/s41467-023-38057-9
76. Jiang C, Zhang L, Li D, Li F. Water discharge and sediment load changes in China: change patterns, causes, and implications. Water. 2015;7(10):5849–5875. https://doi.org/10.3390/w7105849
77. Zhang L, Ssu F, Yang D, Hao Z, Tong K. Discharge regime and simulation for the upstreams of major rivers over Tibetan Plateau. J Geophys Res Atmos. 2013;118(15):8500–8515. https://doi.org/10.1002/jgrd.50665
78. Sarma JN. Water resources of the Brahmaputra: viabilities and apprehensions of its transfer to other rivers. In: Proceedings of the National Seminar on Linking the Major Rivers of India, Possibilities and Apprehensions. Assam Science Society; 2003. https://www.researchgate.net/publication/282866677_WATER_RESOURCES_OF_THE_BRAHMAPUTRA_VIABILITIES_AND_APPREHENSIONS_OF_ITS_TRANSFER_TO_OTHER_RIVER
79. Pangare G, Nishat B, Liao X, Qaddumi HM. The restless river. Washington (DC): World Bank; 2021. https://documents1.worldbank.org/curated/en/267471631520173475/pdf/The-Restless-River-Yarlung-Tsangpo-Siang-Brahmaputra-Jamuna.pdf
80. WAPCOS. Morphological studies of the river Brahmaputra. New Delhi: Northeastern Council, Govt. of India; 1993.
81. Langendoen EJ. CONCEPTS – conservational channel evolution and pollutant transport system, stream corridor version-1(i). Research report no. 16. Oxford (MS): USDA-ARS National Sedimentation Laboratory; 2000. https://www.ars.usda.gov/ARSUserFiles/60600505/TechnicalReports/NSLTechnicalReport16.pdf
82. Pareta K. Two-dimensional morphological model for prediction of erosion of a reach of Brahmaputra River using MIKE 21C software with hydrodynamics and river

morphology modules. River. 2023;2:445–456. https://onlinelibrary.wiley.com/doi/full/10.1002/rvr2.64
83. Bhattacharya NN, Bora AK. Floods of the Brahmaputra River in India. Water Int. 1997;22(4). https://lib.icimod.org/records/gwqhb-h2766
84. Roy NG, Sinha R. Linking hydrology and sediment dynamics of large alluvial rivers to landscape diversity in the Ganga dispersal system, India. Earth Surf Process Landf. 2016;42(7):1078–1091. https://doi.org/10.1002/esp.4074
85. Word JQ, Kauwling TJ, Mearns AJ. A comparative field study of benthic sampling devices. Task report to the US Environmental Protection Agency (EPA Grant No. R801152); 1976.
86. Stubbs HH, Diehl DW, Hershelman GP. A Van Veen grab sampling method. Technical report 276. Southern California Coastal Water Research Project Authority; 1987. https://ftp.sccwrp.org/pub/download/DOCUMENTS/TechnicalReports/0204_VanVeen.pdf
87. Amsterdam EV. Construction materials for civil engineering. Juta and Company Ltd; 2000. p.16.
88. ASCE. Sediment transportation mechanics – sediment discharge formulas. Task Committee for Preparation of Sediment Manual, Committee on Sedimentation of the Hydraulics Division. J Hydraul Div. 1971;97(4). https://ascelibrary.org/doi/abs/10.1061/JYCEAJ.0002933
89. Goswami DC. Brahmaputra River, Assam, India: physiography, basin denudation, and channel aggradation. Water Resour Res. 1985;21(7):959–978. https://doi.org/10.1029/WR021i007p00959
90. Karmakar P, Das PK, Sarkar S, Karmakar S, Mazumdar D. Association study between lead and zinc accumulation at different physiological systems of cattle by canonical correlation and canonical correspondence analyses. Environ Ecol. 2010;28(4):2321–2325.
91. Akbar Z, Pasha GA, Tanaka N, Ghani U, Hamidifar H. Reducing bed scour in meandering channel bends using spur dikes. Int J Sediment Res. 2024;39(2):243–256. https://doi.org/10.1016/j.ijsrc.2024.01.001
92. Koohizadeh Dehkordi A, Fatahi Nafchi R, Samadi-Boroujeni H, Khastar Boroujeni M, Ostad-Ali-Askari K. Assessment of morphological changes of riverbank erosion using Landsat satellite time-series images. Ain Shams Eng J. 2024;15(3):102455. https://doi.org/10.1016/j.asej.2023.102455
93. Zhang GH, Luo RT, Cao Y, Shen RC, Zhang XC. Impacts of sediment load on Manning coefficient in supercritical shallow flow on steep slopes. Hydrol Process. 2010;24(6):3909–3914. https://doi.org/10.1002/hyp.7892
94. Engelund F, Hansen E. A monograph on sediment transport in alluvial streams. Copenhagen: Teknisk Forlag, Danish Technical Press, Danish Technological University; 1967. http://resolver.tudelft.nl/uuid:81101b08-04b5-4082-9121-861949c336c9
95. Benavides-Munoz HM, Roman-Aguilar KM. Hydrodynamic modeling and flood mitigation strategies in an Andean valley city. PLOS Water. 2025;4(7):e0000397. https://doi.org/10.1371/journal.pwat.0000397

© 2025 by the authors. Licensee SCU, Ahvaz, Iran. This article is an open access article distributed under the terms and conditions of the Creative Commons Attribution 4.0 International (CC BY 4.0 license) (http://creativecommons.org/licenses/by/4.0/).